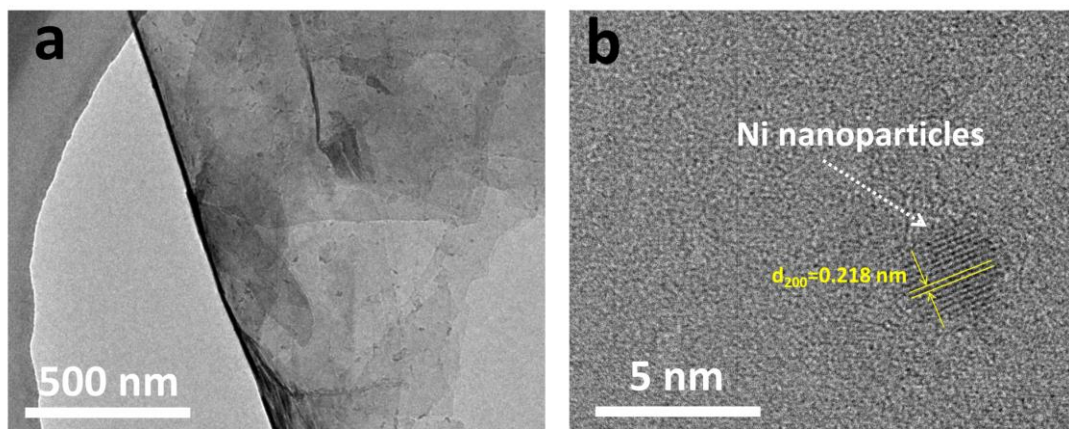


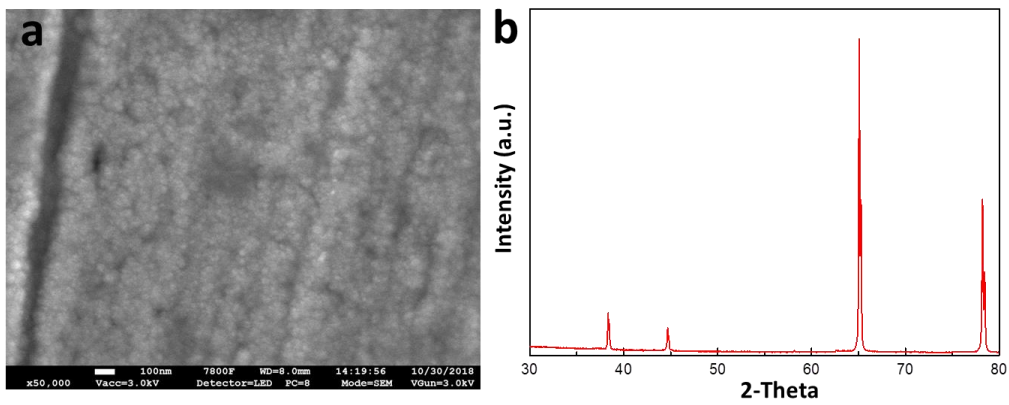
**Selective light absorber-assisted single nickel atom catalysts
for ambient sunlight-driven CO₂ methanation**

Yaguang Li et al.

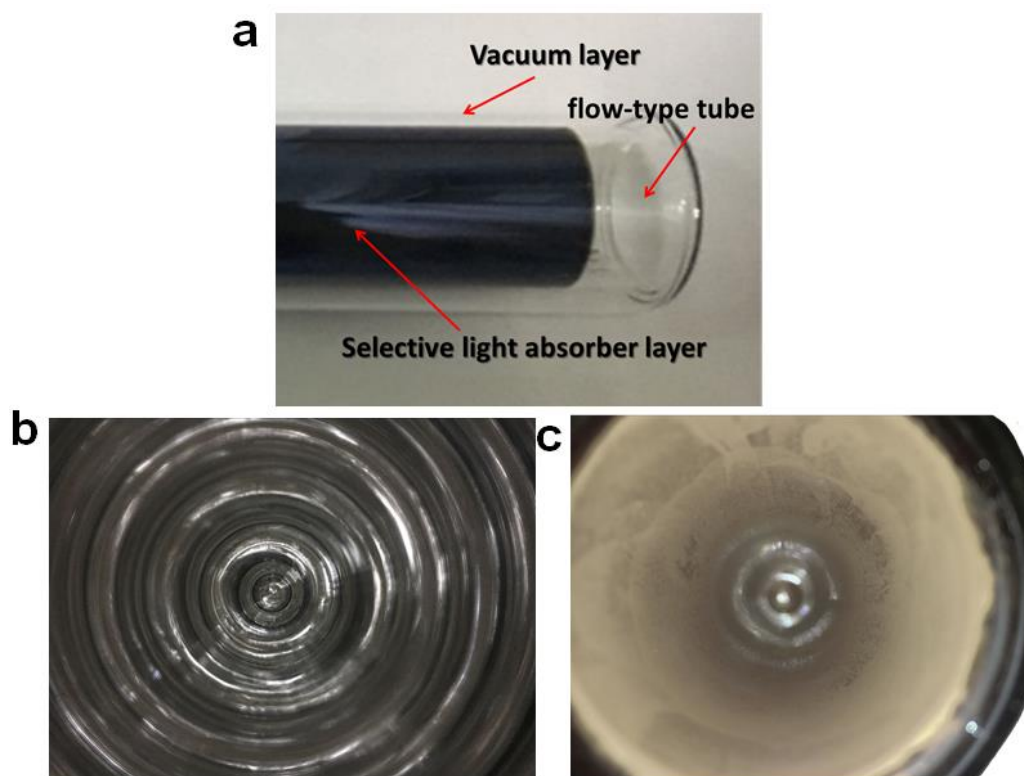


Supplementary Figure 1. Characterization of Ni/Y₂O₃ nanosheets. **a, b** TEM and HRTEM images of Ni/Y₂O₃ nanosheets.

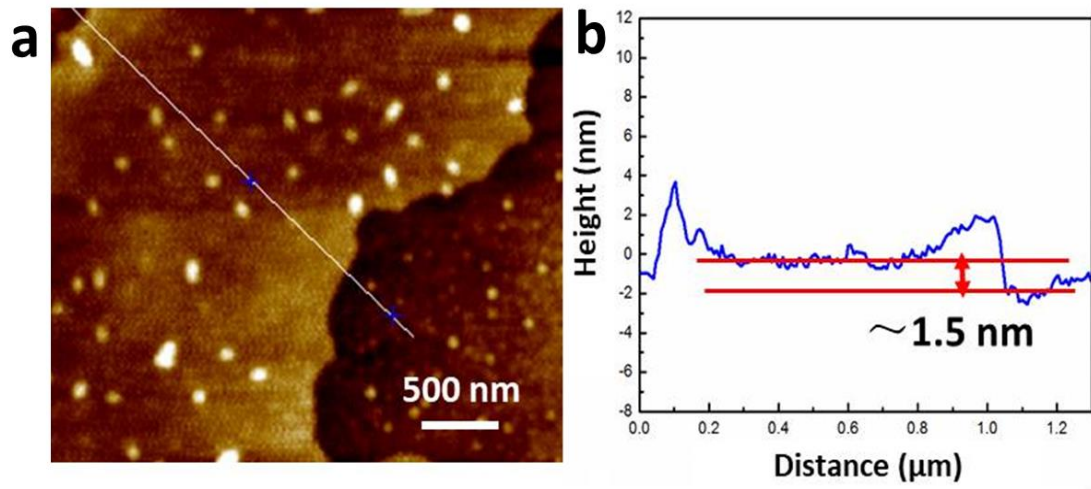
The TEM image of Ni/Y₂O₃ nanosheets showed some nanoparticles distributed on the nanosheets (Supplementary Figure 1a) and the HRTEM image revealed the crystalline nature of the nanoparticles with 0.218 nm of lattice spacing, corresponding to the (002) plane of metallic Ni,¹ thus, confirming that the crystalline precipitations on nanosheets are Ni nanoparticles.



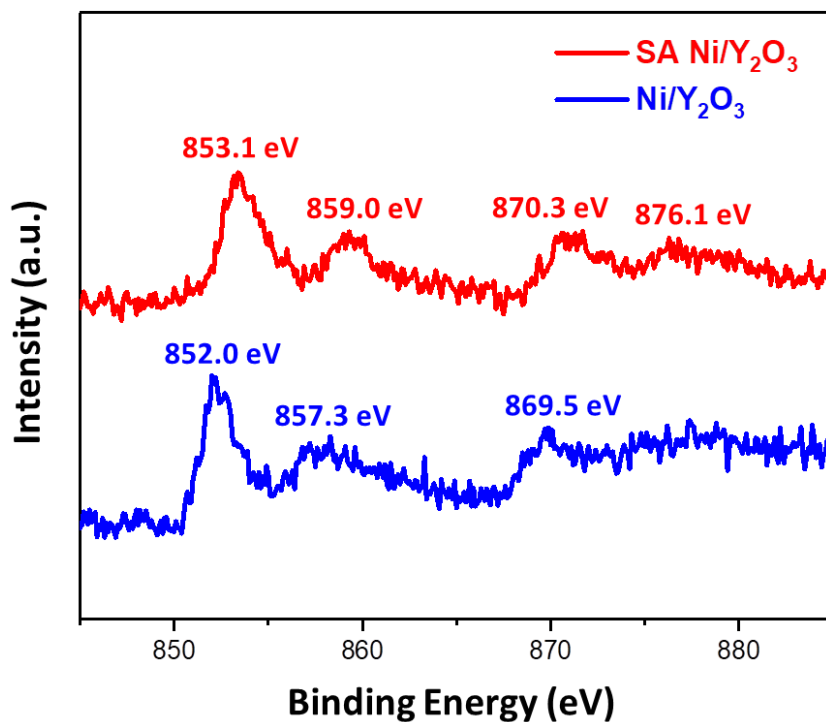
Supplementary Figure 2. Characterization of selective light absorber. **a** SEM image and **b** XRD pattern of selective light absorber.



Supplementary Figure 3. Characterization of selective light absorber coated quartz tube. **a** Photograph of selective light absorber layer coated on quartz tube. **b, c** Photograph of selective light absorber layer assisted quartz tubes coated without and with catalysts.

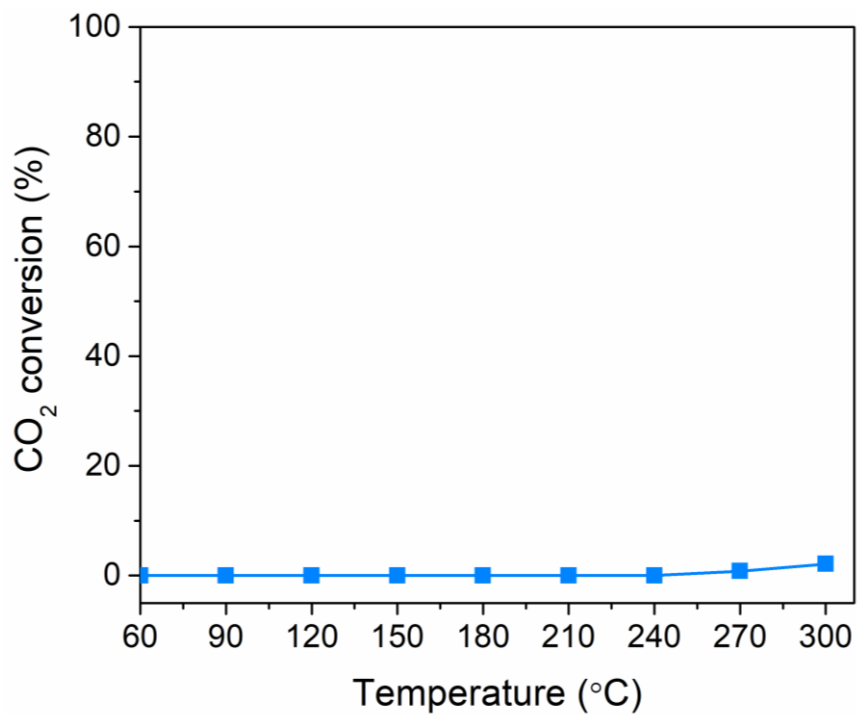


Supplementary Figure 4. Characterization of SA Ni/Y₂O₃ nanosheets. **a** AFM image, **b** height profile of SA Ni/Y₂O₃ nanosheets.

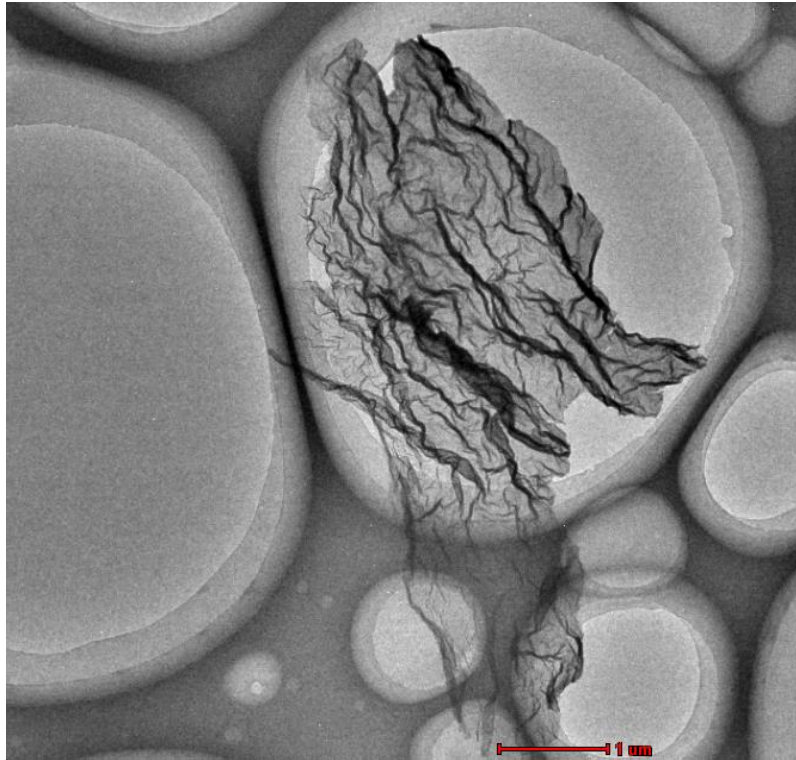


Supplementary Figure 5. The Ni 2p XPS spectra of SA Ni/Y₂O₃ nanosheets (red) and Ni/Y₂O₃ nanosheets (blue).

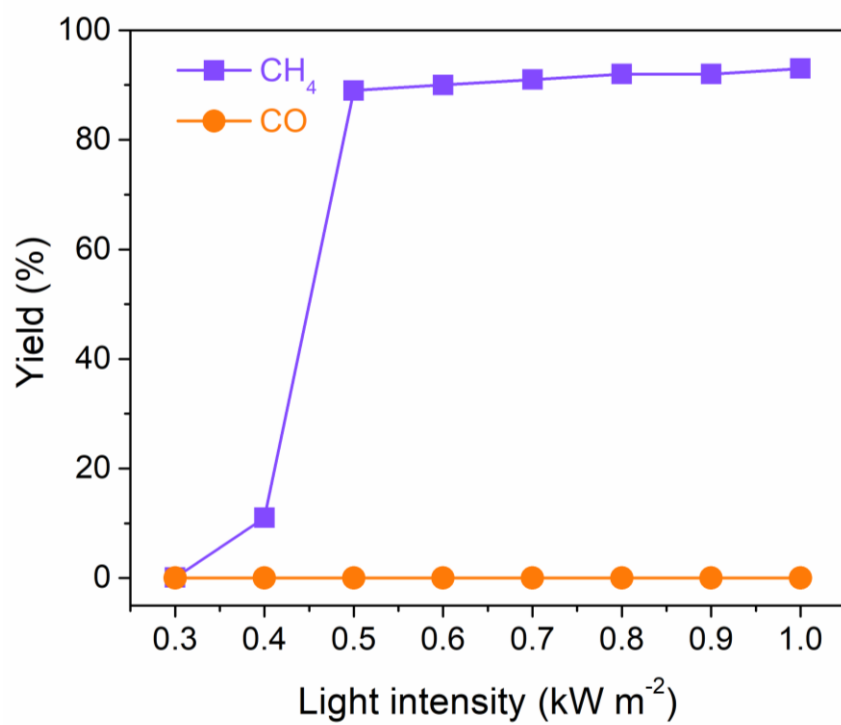
The binding energy of Ni 2p_{3/2} is 853.1 eV for SA Ni/Y₂O₃ nanosheets, a little lower than that of NiO (853.7 eV),¹ revealing the oxidation state of Ni in SA Ni/Y₂O₃ nanosheets. The binding energy of Ni 2p_{3/2} is 852.0 eV for Ni/Y₂O₃ nanosheets, similar to the metallic Ni (852.0 eV),¹ confirming the metallic state of Ni in Ni/Y₂O₃ nanosheets.



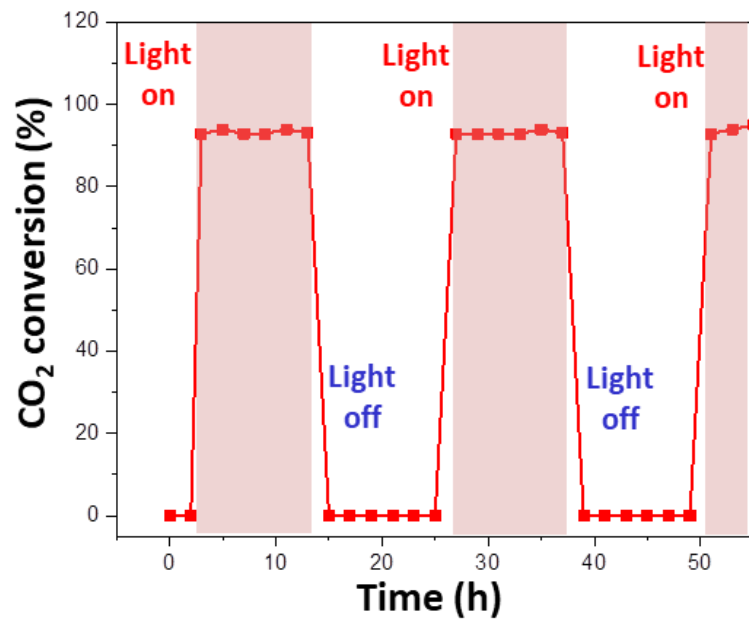
Supplementary Figure 6. Thermal CO₂ conversion of Y₂O₃ nanosheets. Reaction condition: 100 mL min⁻¹ of reaction gas (2.5% CO₂+10 % H₂+ 87.5% N₂), 100 mg of catalysts.



Supplementary Figure 7. TEM image of SA Ni/Y₂O₃ nanosheets after 90 hours' heating/cooling thermal CO₂ methanation test.



Supplementary Figure 8. CH₄ and CO yields in photothermal CO₂ methanation under different densities of solar light irradiation.



Supplementary Figure 9. CO₂ hydrogenation performance versus reaction time, under 1 kW m⁻² of simulated solar light irradiation.

Supplementary Table 1. The sunlight-driven temperature of different materials in air and in vacuum respectively. The sunlight intensity is 1.0 kW m^{-2} .

Materials	CNT	Graphene	2wt% Au/Al ₂ O ₃	4wt% Ni/Y ₂ O ₃	CuO	2wt% Ru/Al ₂ O ₃	Selective light absorber
Temperature in air (°C)	70	79	70	78	82	64	260
Temperature in vacuum (°C)	98	86	88	97	103	82	300

Supplementary Table 2. Physicochemical properties of the as-prepared samples.

Catalysts	Metal loading (wt%) ^a	S _{BET} (m ² g ⁻¹) ^b
3.9 wt% SA Ni/Y ₂ O ₃	3.9	425
Ni/Y ₂ O ₃	4.0	409

a, analyzed by ICP-AES.

b, obtained by N₂ adsorption-desorption method through Brunauer-Emmett-Teller (BET) equation.

Supplementary Table 3. The thermal CO₂ methanation performances of different catalysts.

Catalysts	Temperature (°C)	TOF (CO ₂)	References
SA Ni/Y ₂ O ₃	200	0.023	This work
Ni/Co ₃ O ₄	200	0.003	1
Co NP	200	0.005	2
Ni/Al ₂ O ₃	200	0.006	3
Ni/VO _x	210	0.0023	4
Ni/ZrO ₂	235	0.058	5
Ni/Al ₂ O ₃	300	5.7	6
Ni/SiO ₂	300	1.61	7
Co/ZrO ₂	400	0.2	8
NiFe	300	5.9	9

References

- 1 Wang, Y., Arandiyan, H., Scott, J., Dai, H. & Amal, R. Hierarchically Porous Network-Like Ni/Co₃O₄: Noble Metal-Free Catalysts for Carbon Dioxide Methanation. *Advanced Sustainable Systems* **2**, 1700119 (2018).
- 2 Beaumont, S. K. *et al.* Combining in Situ NEXAFS Spectroscopy and CO₂ Methanation Kinetics To Study Pt and Co Nanoparticle Catalysts Reveals Key Insights into the Role of Platinum in Promoted Cobalt Catalysis. *J. Am. Chem. Soc.* **136**, 9898-9901 (2014).
- 3 Meng, X. *et al.* Photothermal conversion of CO₂ into CH₄ with H₂ over Group VIII nanocatalysts: an alternative approach for solar fuel production. *Angew. Chem. Int. Ed.* **53**, 11478-11482 (2014).
- 4 Lu, X. *et al.* VO_x promoted Ni catalysts supported on the modified bentonite for CO and CO₂ methanation. *Fuel. Process. Technol.* **135**, 34-46 (2015).
- 5 Jia, X., Zhang, X., Rui, N., Hu, X. & Liu, C.-j. Structural effect of Ni/ZrO₂ catalyst on CO₂ methanation with enhanced activity. *Appl. Catal. B-Environ.* **244**, 159-169 (2019).
- 6 He, L., Lin, Q., Liu, Y. & Huang, Y. Unique catalysis of Ni-Al hydrotalcite derived catalyst in CO₂ methanation: cooperative effect between Ni nanoparticles and a basic support. *J. Energy. Chem.* **23**, 587-592 (2014).
- 7 Aziz, M. A. A. *et al.* Highly active Ni-promoted mesostructured silica nanoparticles for CO₂ methanation. *Appl. Catal. B-Environ.* **147**, 359-368 (2014).
- 8 Li, W. *et al.* ZrO₂ support imparts superior activity and stability of Co catalysts for CO₂ methanation. *Appl. Catal. B-Environ.* **220**, 397-408 (2018).
- 9 Pandey, D. & Deo, G. Effect of support on the catalytic activity of supported Ni-Fe catalysts for the CO₂ methanation reaction. *J. Ind. Eng. Chem.* **33**, 99-107 (2016).